

# Dinuclear ruthenium(II) polypyridyl complexes as single and two-photon luminescence cellular imaging probes†

Cite this: *Chem. Commun.*, 2014, 50, 2123Received 22nd November 2013,  
Accepted 23rd December 2013

DOI: 10.1039/c3cc48916g

www.rsc.org/chemcomm

Wenchao Xu, Jiarui Zuo, Lili Wang, Liangnian Ji and Hui Chao\*

**A new series of dinuclear ruthenium(II) polypyridyl complexes, which possess larger  $\pi$ -conjugated systems, good water solubility and pH resistance, and high photostability, were developed to act as single and two-photon luminescence cellular imaging probes.**

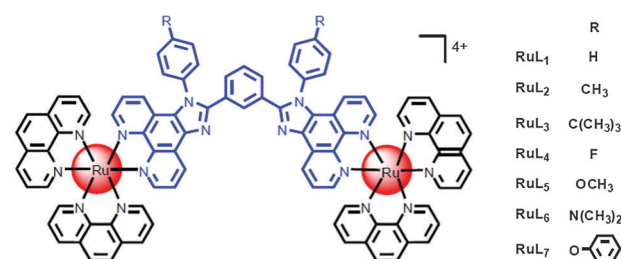
Live cell imaging has been the focus of increasing interest in recent years.<sup>1</sup> As visualisation of cellular events by confocal fluorescence microscopy plays an important role in biochemistry and biomedical research, a wide variety of fluorescent cellular dyes have been developed and utilised, such as the commercial organic dyes 4',6-diamidino-2-phenylindole (DAPI) and MitoTracker Green. However, most of the commercially available dyes have notable shortcomings including poor water solubility, high toxicity to living cells and poor photostability. These commercial organic dyes may also cause extensive cellular damage and unwanted background signals due to the ultraviolet (UV) radiation required for their excitation and small Stokes shifts.<sup>2</sup> These short excitation wavelengths (< 650 nm) also inhibit the application of these materials in thick tissues or live animals due to the resultant short penetration depth.<sup>3</sup> The use of two-photon fluorescence probes is an attractive solution to these problems because these molecules exhibit near infrared (NIR) or longer excitation wavelengths, less phototoxicity, deeper penetration depth and reduction of photobleaching.<sup>4</sup> As such, many laboratories are focused on the development of new two-photon imaging probes, such as organic dyes,<sup>5</sup> luminescent d<sup>6</sup>-metal complexes (e.g., complexes of Ir and Re),<sup>6</sup> d<sup>8</sup>-metal Pt complexes,<sup>7</sup> d<sup>10</sup>-metal Zn(II) salen complexes<sup>8</sup> and quantum dots.<sup>9</sup> However, rationally designed molecules providing efficient two-photon absorption (TPA) medium compatibility, photostability, membrane-crossing capabilities and low cytotoxicity are still highly sought.

In this work, we focus on Ru(II) polypyridyl complexes, not only because of their outstanding photochemical properties,

such as their exceptional nonlinear optical properties, high luminescence, large Stokes shifts, high photostability and relatively long lifetimes, but also because of their small molecular weight, enabling easy penetration of cell membranes for live cell staining processes.<sup>10</sup> Recently, some Ru(II) polypyridyl complexes have been investigated for applications in live cell imaging;<sup>11</sup> however, only a few were successfully applied as two-photon luminescent cellular imaging probes.<sup>12</sup> The vast potential of Ru(II) complexes as two-photon imaging probes remains largely untapped. In the present work, we synthesised a series of dinuclear Ru(II) polypyridyl complexes, [(phen)<sub>2</sub>Ru(L<sub>1-7</sub>)Ru(phen)<sub>2</sub>]<sup>4+</sup> (**RuL<sub>1-7</sub>**, phen = 1,10-phenanthroline, L = 1,3-bis(1-substituted-1*H*-imidazo[4,5-*f*][1,10]phenanthroline-2-yl)-benzene), which possess larger  $\pi$ -conjugated systems, good water solubility and pH resistance, high photostability, and proved to be useful as single and two-photon luminescent cellular imaging probes.

The syntheses of **RuL<sub>1-7</sub>** (Scheme 1) were accomplished as described in Scheme S1 (ESI†). The bridging ligands were synthesised through the condensation of 1,10-phenanthroline-5,6-dione, isophthalic aldehyde, 4-substituted aniline and ammonium acetate in refluxing glacial acetic acid over 24 h. The Ru(II) complexes were obtained in yields ranging from 56% to 68% by the direct reaction of **L<sub>1-7</sub>** with appropriate molar ratios of *cis*-Ru(phen)<sub>2</sub>Cl<sub>2</sub> in ethylene glycol. The synthetic details and characterisation data for these complexes are provided in Fig. S1–S21, ESI.†

We studied the electronic absorption and emission spectra of **RuL<sub>1-7</sub>** in aqueous media (DMSO–H<sub>2</sub>O, v/v = 1 : 99) at 298 K

Scheme 1 The chemical structure of complexes **RuL<sub>1-7</sub>**.

MOE Key Laboratory of Bioinorganic and Synthetic Chemistry, State Key Laboratory of Optoelectronic Materials and Technologies, School of Chemistry and Chemical Engineering, Sun Yat-Sen University, Guangzhou 510275, P. R. China.

E-mail: ceschh@mail.sysu.edu.cn; Fax: +86-20-84112245; Tel: +86-20-84110613

† Electronic supplementary information (ESI) available: Procedures and additional experiments. See DOI: 10.1039/c3cc48916g

(Table S1, ESI†). All of the complexes showed good solubility. **RuL**<sub>1-7</sub> each show intense absorption features ( $\epsilon$  on the order of  $10^4 \text{ M}^{-1} \text{ cm}^{-1}$ ) between 230 nm and 600 nm (Fig. S22, ESI†). The emission spectra of **RuL**<sub>1-7</sub> exhibit  $\lambda_{\text{em}}$  values at approximately 603 nm with quantum yields ( $\phi$ ) of 0.041–0.054, using  $[\text{Ru}(\text{bpy})_3]^{2+}$  as a standard<sup>13</sup> (Fig. S23, ESI†). A luminescence decay experiment performed at room temperature determined the lifetimes of **RuL**<sub>1-7</sub> to be  $\sim 987$ – $1114$  ns through fitting the data to a single exponential decay function. The Stokes shifts of **RuL**<sub>1-7</sub> were measured to be  $\sim 146$ – $153$  nm. These large Stokes shifts offer advantages over popular commercial cellular dyes such as DAPI (Stokes shift = 46 nm) or SYTO-17 (Stokes shift = 18 nm).<sup>14</sup>

The two-photon absorption (TPA) properties of **RuL**<sub>1-7</sub> were also studied. With reference to rhodamine B,<sup>15</sup> the largest two-photon absorption cross-sections ( $\delta$ ) of **RuL**<sub>1-7</sub> were estimated to be 322–386 Göppert-Mayer (GM) units ( $1 \text{ GM} = 1 \times 10^{-50} \text{ cm}^4 \text{ s}^{-1} \text{ photon}^{-1}$ ) (Table S1, Fig. S24 and S25, ESI†), hundreds of times larger than those of commercially available dyes used in two-photon excited (TPE) microscopy ( $0.16 \text{ GM}$  for DAPI and  $1 \text{ GM}$  for Cascade Blue fluorescent dyes<sup>15a</sup>) and significantly larger than some recently reported two-photon bio-available organometallic molecular probes.<sup>1c,6-8</sup>

High cell viability is essential for biological applications. Cell viability assays using HeLa cells were conducted *via* the 3-(4,5-dimethylthiazol-2-yl)-2,5-diphenyltetrazolium bromide (MTT) assay. Fig. S26 (ESI†) shows that **RuL**<sub>1-7</sub> all demonstrated high cell viability over a 24 hour incubation period at several concentrations (from  $5 \mu\text{M}$  to  $20 \mu\text{M}$ ). This indicates that **RuL**<sub>1-7</sub> each presented low toxicity during luminescence cell imaging under the applied conditions (incubation times of 2 h, ruthenium complex concentrations of  $10 \mu\text{M}$ ). To investigate the application of **RuL**<sub>1-7</sub> in living cell imaging, the uptake of **RuL**<sub>1-7</sub> by HeLa cells was evaluated. Confocal microscopy images showed efficient uptake of **RuL**<sub>1-7</sub> (initial concentration =  $10 \mu\text{M}$ ) by HeLa cells within 2 h (Fig. 1a and Fig. S27a–S32a, ESI†). The Ru(II) complexes were functionalised with different substituents with the expectation that different dyes may reside in different locations within the live cell. Unexpectedly, there were only small differences between the **RuL**<sub>1-7</sub> complexes in this respect, so **RuL**<sub>4</sub> was chosen as the model complex in the next several experiments. To demonstrate the advantage of using **RuL**<sub>1-7</sub> as two-photon luminescence cellular dyes in living cells, we

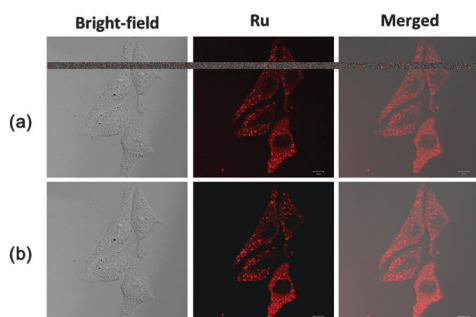


**Fig. 1** OPM (a) and TPM (b) images of HeLa cells incubated with **RuL**<sub>4</sub> ( $10 \mu\text{M}$ ) for 2 h at  $37^\circ\text{C}$ . The wavelengths for one- and two-photon excitation were 458 and 830 nm, respectively.

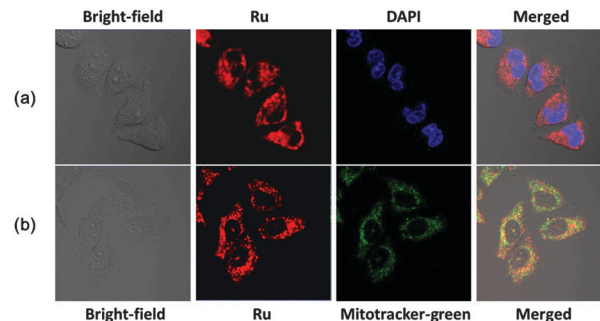


**Fig. 2** OPM images of living HeLa cells incubated with  $10 \mu\text{M}$  **RuL**<sub>4</sub> for 2 h at  $37^\circ\text{C}$  and then further incubated with DAPI (a) and MitoTracker Green (b).

conducted two-photon fluorescence microscopy (TPM) imaging experiments (Fig. S27b–32b, ESI†). The TPM images of HeLa cells stained with **RuL**<sub>4</sub> (Fig. 1b) showed similarities with OPM (one-photon fluorescence microscopy) images, confirming penetration of the dye into the cell cytoplasm. Due to the two-photon absorption, the background signal was strongly suppressed, resulting in a TPM image of higher resolution and better signal to noise contrast.

To determine the location of the probes within the cells, co-localisation studies of **RuL**<sub>4</sub> with several well-known one-photon fluorescence probes were conducted in HeLa cells. The OPM images of HeLa cells co-stained with **RuL**<sub>4</sub> and DAPI or MitoTracker Green (Fig. 2) individually demonstrated that the localisation of **RuL**<sub>4</sub> in the cells was similar to that of MitoTracker Green, but not identical. To better understand the location of the dye in the cell, a z-stack experiment (three-dimensional visualisation) was processed. HeLa cells were co-stained with MitoTracker Green and **RuL**<sub>4</sub> and imaged by serially scanning at increasing depths along the z-axis. Fig. 3 shows that in *xy* images of the cells obtained at a depth *z*, most of the cell cytoplasm was stained green with MitoTracker Green and red with **RuL**<sub>4</sub> (the overlap was yellow), but the nuclear regions were blank. Images involving co-localisation with MitoTracker Green clearly showed that the observed luminescence was evenly distributed throughout the cytoplasm, but excluded from the nucleus. Inductively coupled plasma mass spectrometry (ICP-MS) experiments were carried out to quantify the amounts of ruthenium in the nucleus and the cytoplasm of a RuL-stained cell.

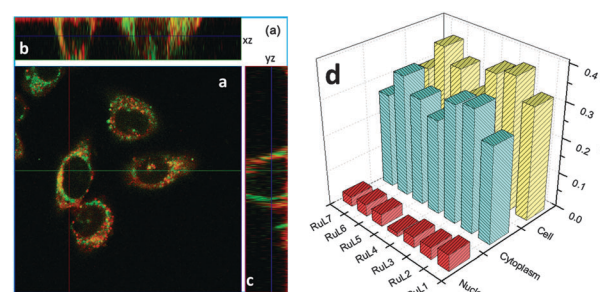


**Fig. 3** Three-dimensional luminescence images of live HeLa cells incubated with  $10 \mu\text{M}$  **RuL**<sub>4</sub> for 2 h at  $37^\circ\text{C}$ . The cells were co-stained green with MitoTracker Green. Panel (a) shows an *xy* image obtained at  $z = 8.4 \mu\text{m}$ , while panels (b) and (c) display the *xz* and *yz* cross sections ( $z = 1.3$ – $18.9 \mu\text{m}$ ) taken at the lines shown in panel (a), respectively. (d) The distribution analysis of **RuL**<sub>1-7</sub> in HeLa cells by ICP-MS.

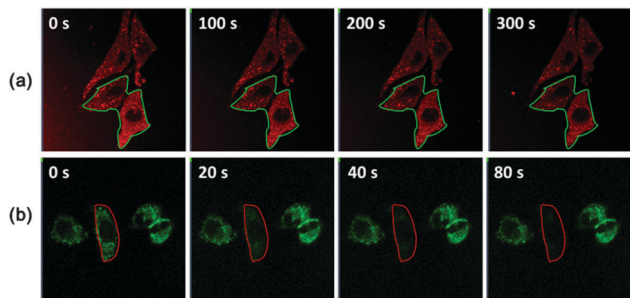


Fig. 4 Photostability comparison of **RuL<sub>4</sub>** and MitoTracker Green in HeLa cells. (a) and (b) OPM images of HeLa cells stained with **RuL<sub>4</sub>** and MitoTracker Green, respectively. The images were taken under successive irradiation. The wavelengths for **RuL<sub>4</sub>** and MitoTracker Green irradiation were 458 and 488 nm, respectively.

As expected, the results showed a substantial difference between the nucleus ( $\sim 0.03$  pg Ru per cell) and the cytoplasm ( $\sim 0.3$  pg Ru per cell), suggesting that more than 90% of the ruthenium was distributed in the cell cytoplasm (Fig. 3d).

To further explore the application of Ru(II) complexes as cellular dyes, the photostabilities of **RuL<sub>1-7</sub>** were examined in comparison to commercially available MitoTracker Green in living HeLa cells *via* photobleaching experiments. Fig. 4 shows that the fluorescence intensity of MitoTracker Green decreased 80% after 80 s (and 93% for 300 s) of irradiation. In contrast to this nearly complete photobleaching, the fluorescence intensity of **RuL<sub>4</sub>** decreased only 38% after 300 s of irradiation, suggesting greater photostability of **RuL<sub>4</sub>** in comparison to MitoTracker Green. Similar results were observed for other Ru(II) complexes (Fig. S33 and S34, ESI<sup>†</sup>). For biological applications of a dye, it should operate in a wide pH range. The effect of pH on the luminescent response of **RuL<sub>1-7</sub>** was investigated. The pH titration curve revealed that the luminescence intensity was barely affected when the pH was varied from 4–10 (Fig. S35, ESI<sup>†</sup>).

We then decided to investigate the mechanism of cellular uptake of the Ru complex using confocal microscopy (Fig. S36, ESI<sup>†</sup>) and flow cytometry (Fig. S37, ESI<sup>†</sup>). To determine whether **RuL<sub>4</sub>** entered the cell *via* an energy-dependent or energy-independent transport pathway, HeLa cells were either incubated with **RuL<sub>4</sub>** at 4 °C or pretreated with the metabolic inhibitors 2-deoxy-D-glucose and oligomycin.<sup>16</sup> Fig. S36b and c (ESI<sup>†</sup>) show that cellular luminescence was significantly suppressed in cases when the cells were incubated with the complex at 4 °C or pretreated with the metabolic inhibitors, indicating that **RuL<sub>4</sub>** uptake followed an energy-dependent pathway. Endocytosis is well known as the most common energy-dependent pathway by which eukaryotic cells uptake extracellular materials. Endocytosis is also affected by temperature or adenosine triphosphate (ATP). We used the endocytic inhibitors chloroquine and NH<sub>4</sub>Cl to examine the role of this pathway in **RuL<sub>4</sub>** uptake. After treatment with these inhibitors (Fig. S36d and e, ESI<sup>†</sup>), no significant suppression of luminescence was observed, suggesting that endocytosis was not responsible for the uptake of **RuL<sub>4</sub>**. This is not surprising because cellular uptake mechanisms are generally complex and diverse.

In conclusion, we have designed and synthesized a new series of dinuclear Ru(II) polypyridyl complexes (**RuL<sub>1-7</sub>**) that

proved to be effective as single and two-photon luminescence cellular imaging dyes. Fluorescence microscopy imaging and ICP-MS revealed that most of the novel ruthenium complexes stained the cell cytoplasm, rather than the nucleus. Due to their low cytotoxicities to living cells, photostabilities, pH resistance, membrane permeabilities, and especially their large two-photon absorption cross sections, **RuL<sub>1-7</sub>** are believed to have great potential as biocompatible dyes for living cells both in OPM and TPM imaging. These novel dinuclear ruthenium complexes provide a platform for the design of new TPM imaging dyes.

This project was financially supported by NSFC (21071155, 21172273, 21171177, 91122010, J1103305), the 973 Program (2014CB845604), and the Program for Changjiang Scholars and Innovative Research Team at the University of China (No. IRT1298).

## Notes and references

- (a) T. Terai and T. Nagano, *Curr. Opin. Chem. Biol.*, 2008, **12**, 515; (b) M. Y. Berezin and S. Achilefu, *Chem. Rev.*, 2010, **110**, 2641; (c) Y. M. Yang, Q. Zhao, W. Feng and F. Y. Li, *Chem. Rev.*, 2013, **113**, 192.
- G. P. Pfeifer, Y. H. You and A. Besaratinia, *Mutat. Res.*, 2005, **571**, 19.
- W. R. Zipfel, R. M. Williams and W. W. Webb, *Nat. Biotechnol.*, 2003, **21**, 1369.
- U. K. Tirlapur and K. Konig, *Nature*, 2002, **418**, 290.
- (a) H. M. Kim and B. R. Cho, *Acc. Chem. Res.*, 2009, **42**, 863; (b) M. Pawlicki, H. A. Collins, R. G. Denning and H. L. Anderson, *Angew. Chem., Int. Ed.*, 2009, **48**, 3244; (c) S. Yao and K. D. Belfield, *Eur. J. Org. Chem.*, 2012, 3199; (d) B. Dumat, G. Bordeaux, E. Faurel-Paul, F. Mahuteau-Betzer, N. Saettel, G. Metge, C. Fiorini-Debuisschert, F. Charra and M.-P. Teulade-Fichou, *J. Am. Chem. Soc.*, 2013, **135**, 12697; (e) H. Zhang, J. Fan, J. Wang, S. Zhang, B. Dou and X. Peng, *J. Am. Chem. Soc.*, 2013, **135**, 11663; (f) S. K. Bae, C. H. Heo, D. J. Choi, D. Sen, E.-H. Joe, B. R. Cho and H. M. Kim, *J. Am. Chem. Soc.*, 2013, **135**, 9915.
- Q. Zhao, C. Huang and F. Li, *Chem. Soc. Rev.*, 2011, **40**, 2508.
- (a) S. Botchway, M. Charnley, J. Haycock, A. Parker, D. Rochester, J. Weinstein and J. Williams, *Proc. Natl. Acad. Sci. U. S. A.*, 2008, **105**, 16071; (b) C. K. Koo, K. L. Wong, C. W. Y. Man, Y. W. Lam, K. Y. So, H. L. Tam, S. W. Tsao, K. W. Cheah, K. C. Lau, Y. Y. Yang, J. C. Chen and M. H. W. Lam, *Inorg. Chem.*, 2009, **48**, 872; (c) C. K. Koo, L. K. Y. So, K. L. Wong, Y. M. Ho, Y. W. Lam, M. H. W. Lam, K. W. Cheah, C. C. W. Cheng and W. M. Kwok, *Chem.-Eur. J.*, 2010, **16**, 3942.
- (a) Y. Hai, J. J. Chen, P. Zhao, H. Lv, Y. Yu, P. Xu and J. L. Zhang, *Chem. Commun.*, 2011, **47**, 2435; (b) J. Jing, J. Chen, Y. Hai, J. Zhan, P. Xu and J. L. Zhang, *Chem. Sci.*, 2012, **3**, 3315.
- (a) D. R. Larson, W. R. Zipfel, R. M. Williams, S. W. Clark, M. P. Bruchez, F. W. Wise and W. W. Webb, *Science*, 2003, **300**, 1434; (b) X. Michalet, F. F. Pinaud, L. A. Bentolila, J. M. Tsay, S. Doose, J. J. Li, G. Sundaresan, A. M. Wu, S. S. Gambhir and S. Weiss, *Science*, 2005, **307**, 538; (c) L. Cao, X. Wang, M. J. Meziani, F. S. Lu, H. F. Wang, P. J. G. Luo, Y. Lin, B. A. Harruff, L. M. Veca, D. Murray, S. Y. Xie and Y. P. Sun, *J. Am. Chem. Soc.*, 2007, **129**, 11318; (d) S. K. Chakraborty, J. A. J. Fitzpatrick, J. A. Phillippi, S. Andreko, A. S. Waggoner, W. P. Bruchez and B. Ballou, *Nano Lett.*, 2007, **7**, 2618.
- V. Fernández-Moreira, F. Thorp-Greenwood and M. P. Coogan, *Chem. Commun.*, 2010, **46**, 186.
- M. R. Gill and J. A. Thomas, *Chem. Soc. Rev.*, 2012, **41**, 3179.
- (a) S. C. Boca, M. Four, A. Bonne, B. van der Sanden, S. Astilean, P. L. Baldeck and G. Lemerrier, *Chem. Commun.*, 2009, 4590; (b) H. Ke, H. Wang, W.-K. Wong, N.-K. Mak, D. W. J. Kwong, K.-L. Wong and H.-L. Tam, *Chem. Commun.*, 2010, **46**, 6678; (c) P. Zhang, L. Pei, Y. Chen, W. Xu, Q. Lin, J. Wang, J. Wu, Y. Shen, L. Ji and H. Chao, *Chem.-Eur. J.*, 2013, **19**, 15494.
- K. Nakamaru, *Bull. Chem. Soc. Jpn.*, 1982, **55**, 2697.
- R. P. Haugland, in *Handbook of Fluorescent Probes and Research Chemicals*, ed. M. T. Z. Spence, Molecular Probes Inc., Eugene, 1996, p. 144.
- (a) C. Xu and W. W. Webb, *J. Opt. Soc. Am. B*, 1996, **13**, 481; (b) N. S. Makarov, M. Drobizhev and A. Rebane, *Opt. Express*, 2008, **16**, 4029.
- C. A. Puckett and J. K. Barton, *Biochemistry*, 2008, **47**, 11711.